IEEE Access
Multidisciplinary ⋮ Rapid Review ⋮ Open Access Journal

Received 9 October 2023, accepted 28 October 2023, date of publication 1 November 2023, date of current version 7 November 2023.

Digital Object Identifier 10.1109/ACCESS.2023.3329060

RESEARCH ARTICLE

Robust Control of Autonomous Underwater Vehicles Using Delta-Sigma-Based 1-bit Controllers

CHATHURA WANIGASEKARA[1], (Member, IEEE), FRANK SILL TORRES[1], (Senior Member, IEEE), AND AKSHYA SWAIN[2], (Senior Member, IEEE)

[1]Institute for the Protection of Maritime Infrastructures, German Aerospace Center (DLR), 27572 Bremerhaven, Germany
[2]Department of Electrical, Computer, and Software Engineering, The University of Auckland, Auckland 1010, New Zealand

Corresponding author: Chathura Wanigasekara (chathura.wanigasekara@dlr.de)

This work was supported by the German Aerospace Centre (DLR).

ABSTRACT Autonomous underwater vehicles (AUVs) are robots capable of operating underwater without the need for human operators. Nonetheless, there is the essential requirement of remote operation capability in case of exceptional situations, such as the encounter of unforeseen obstacles or malfunctions. The corresponding robust controller design is a challenging task, especially due to limited communication bandwidth to the land based control system as well as the exposure to disturbances like water currents. The present study, therefore, proposes a Delta-Sigma-based **1**-bit PID controller for such AUVs, which consumes less communication resources and is robust to various disturbances arising in the underwater environment. The proposed controller is designed using the Takagi-Sugeno (T-S) fuzzy model of the nonlinear AUV systems. A comparative performance investigation of this controller is carried out with an output feedback controller as reference design, which is based on the same T-S fuzzy model. The stability conditions of both controllers are established. Obtained simulation results indicate that in case of extreme disturbances and limited bandwidth, the reference controller could not stabilise the AUV system. In contrast, the proposed Delta-Sigma-based **1**-bit PID controller performed well under all conditions, while using less hardware and communication resources compared to the reference design.

INDEX TERMS T-S fuzzy systems, 1-bit control, autonomous under water vehicles.

I. INTRODUCTION

During the past decade, autonomous underwater vehicles (AUV) have attracted notable attention due to its ability to operate autonomously in situations difficult or impossible for human divers, improvements in sensors technologies and propulsion systems leading to more efficient and reliable operations, and increasing accessibility following from reducing costs and easier operability [1]. Consequently, AUVs are widely used in applications such as deep-sea exploration, resource and area monitoring, military operations, etc.

Despite the fact that AUVs are designed to operate without direct human control and to carry out missions independently, they still require the capability to be remotely controlled in exceptional situations. This includes, for example, the encounter of unforeseen obstacles or the occurrence of system malfunctions. Additional purposes for remote control can be fine-tuning of the AUV operation and real-time adjustments to the mission plan.

However, remote control of AUV is a challenging task resulting from its exposure to the harsh maritime environment and limited underwater communication [2]. For successful local navigation of AUVs, various researchers have proposed different control strategies for motion control of AUVs, such as dynamic position control, trajectory tracking control, path following control, heading control, etc. [3], [4].

The associate editor coordinating the review of this manuscript and approving it for publication was Min Wang.

Following from advancement of communication technologies in recent years, the land based control of AUV is becoming increasingly popular [2], [5], [6], [7]. This strategy is similar to the networked control systems (NCSs) framework which is widely employed by control engineers [8], [9]. NCSs are also cyber-physical systems and offer advantages like easy operation, low effort system diagnosis, increase in system agility, convenience and reduces system wiring [10], [11]. However, having a communication channel in the control loop can cause various other problems such as delay in signals, quantisation errors and packet losses due to network constraints. In underwater environment, these are further aggravated by high signal attenuation.

One of the effective methods to represent highly nonlinear systems such as AUV systems is using T-S fuzzy models, which have been proven to be very effective [12]. It could be shown that the T-S fuzzy model is an universal approximator for a wide class of nonlinear systems, which are represented via a group of linear models and membership functions [13], [14], [15], [16]. Motivated by this, T-S fuzzy models have been applied extensively for modelling and control of AUV systems [1]. For example, T-S fuzzy model have been used to design a fault-tolerant control strategy to solve thruster fault related problems [17] and to solve tracking control problem using adaptive control and sliding mode control [18]. However, to the best of our knowledge, no T-S fuzzy model that explicitly addresses the robust control problem associated with AUV systems has been reported.

Especially in security related scenarios, there is the risk that AUV communication is subjected to malicious attacks such as *deception attack*, *denial of service (DoS) attack*, *congestion attack* and similar [19]. When AUVs, which are controlled by land based control strategies, are subjected to congestion attacks, the communication resources are severely impaired and its control becomes a challenging task. At low levels of congestion, this problem can be solved using high-bit quantisers such as neural network quantisers, logarithmic quantisers, nearest neighbour quantisers [20], [21], [22], [23], [24], [25]. However, these quantisers consume more bandwidth and become ineffective and, in case of severe congestion attacks, can even turn the system unstable [26].

The principal goal of the present study is to address the problem of limited bandwidth for remote control of AUVs. One of the captivating ways of solving the bandwidth utilisation problem related to high-bit quantisers is through **1**-bit quantisers. There are several **1**-bit quantisers, such as Delta-Sigma Modulator, Sigma-Delta Modulator, Delta-Modulator, and Hybrid-Delta Modulator [11], [27], [28], [29], [30], [31]. These **1**-bit quantisers are integrated with different control strategies to form **1**-bit controllers, which are also referred as bit-stream controllers [32], [33]. Despite the fact that these types of modulators consume significantly less hardware resources and could minimise the quantisation error, this study focuses on Delta-Sigma modulator based controllers following from their excellent anti-aliasing capabilities and high resolution [30].

Thus, we develop a Delta-Sigma-based **1**-bit controller for the robust control of a nonlinear AUV system in the presence of network constraints and disturbances. Furthermore, an output feedback controller for the AUV system is designed as reference to compare the performance of the Delta-Sigma-based **1**-bit controller. This papers' primary contributions can be summed up as follows:

1) Design of a Delta-Sigma-based **1**-bit controller for nonlinear systems represented by T-S fuzzy model with special emphasis on AUV systems.
2) Establishment of stability conditions for the Delta-Sigma-based **1**-bit controller.
3) For comparative performance investigation, design of an output feedback controller for T-S fuzzy AUV systems and derivation of its stability conditions.
4) Validation of the performance of the proposed controller via simulations, considering multiple disturbance scenarios of varying intensities, which commonly arise in underwater environment.

The rest of the paper is organised as follows. Section-II describes the dynamics of autonomous underwater vehicle and the T-S fuzzy model. Section-III and Section-IV discuss the design procedures of the Delta-Sigma-based **1**-bit controller and the output feedback controller, respectively. In Section-V, simulation of an AUV example is used to verify the efficacy of the suggested control schemes and the theoretical findings. This is followed by conclusions in Section-VI.

Preliminaries: For the rest of the paper, Euclidean norm is used for vectors. The transpose and inverse of any matrix Π is denoted by Π^T and Π^{-1}. Negative semi-definite, negative definite, positive semi-definite, and positive definite matrices of Π is represented using $\Pi \leq 0$, $\Pi < 0$, $\Pi \geq 0$ and $\Pi > 0$, respectively. The identity and zero matrices of appropriate dimensions are denoted by $\boldsymbol{I}$ and $\boldsymbol{0}$. The dimensions of matrices are considered to be consistent with algebraic operations if they are not specified in the text. Any term that is induced by the symmetry is represented by the symbol $\star$.

II. T-S FUZZY MODEL OF AUTONOMOUS UNDERWATER VEHICLE (AUV)

The dynamics of the AUV system can be described using yaw, sway and surge velocities as [1]:

$$1\mathcal{M}\dot{\mathcal{V}}(t) + \mathcal{N}\mathcal{V}(t) + \mathcal{G}\Omega(t) = \mathcal{U}(t) \tag{1a}$$

$$\dot{\Omega}(t) = \mathcal{R}\left[\phi(t)\right]\mathcal{V}(t) \tag{1b}$$

where $\mathcal{V}(t)$ is the body-fixed velocities vector, $\Omega(t)$ denotes the earth-fixed orientation vector, $\mathcal{U}(t)$ represents the control vector, $\mathcal{M}$ means the inertia matrix, $\mathcal{N}$ is the damping matrix, and $\mathcal{G}$ represents the mooring matrix. Furthermore:

$$\mathcal{V}(t) = \left[\mathcal{V}_1^T(t)\ \mathcal{V}_2^T(t)\ \mathcal{V}_3^T(t)\right]^T$$
$$\Omega(t) = \left[\mathcal{X}_p^T(t)\ \mathcal{Y}_p^T(t)\ \phi^T(t)\right]^T$$
$$\mathcal{U}(t) = \left[\mathcal{U}_1^T(t)\ \mathcal{U}_2^T(t)\ \mathcal{U}_3^T(t)\right]^T$$
$$\mathcal{M} = \mathcal{M}^T > 0$$
$$\mathcal{G} = diag\{\mathcal{G}_{1,1}, \mathcal{G}_{2,2}, \mathcal{G}_{3,3}\}$$
$$\mathcal{R}[\phi(t)] = \begin{bmatrix} \cos[\phi(t)] & -\sin[\phi(t)] & 0 \\ \sin[\phi(t)] & \cos[\phi(t)] & 0 \\ 0 & 0 & 1 \end{bmatrix}. \tag{2}$$

The dynamics of an AUV, described in (1a), can be reformulated as:

$$\dot{\mathcal{V}}(t) = \mathcal{A}\mathcal{V}(t) + \mathcal{B}\Omega(t) + \mathcal{D}\mathcal{U}(t) \tag{3}$$

where $\mathcal{A} = -\mathcal{M}^{-1}\mathcal{N}$, $\mathcal{B} = -\mathcal{M}^{-1}\mathcal{G}$ and $\mathcal{D} = \mathcal{M}^{-1}$.

Define that $\mathcal{X}(t) = [\mathcal{V}^T(t)\ \Omega^T(t)]^T$. Then, the state space model of the AUV system can be formulated using (1) and (3) as:

$$\dot{\mathcal{X}}(t) = \bar{\mathcal{A}}(\phi(t))\mathcal{X}(t) + \bar{\mathcal{B}}\mathcal{U}(t) \tag{4}$$

where

$$\bar{\mathcal{A}}[\phi(t)] = \begin{bmatrix} 0_{3\times3} & \mathcal{R}(\phi(t)) \\ \mathcal{B} & \mathcal{A} \end{bmatrix}, \bar{\mathcal{B}} = \begin{bmatrix} 0_{3\times3} \\ \mathcal{D} \end{bmatrix}.$$

Define $\xi_1(t) = \sin[\phi(t)]$, and $\xi_2(t) = \cos[\phi(t)]$. In this study, the yaw angle $\phi(t)$ is assumed to be in the interval $[-\pi/6, \pi/6]$. Hence, $\xi_1(t) \in [-1/2, 1/2]$ and $\xi_2(t) \in [\sqrt{3}/2, 1]$. The T-S fuzzy AUV model can be described using following rules:

Plant Rule i:

IF $\xi_1(t)$ is $\mathcal{F}_{i1}$ and $\xi_2(t)$ is $\mathcal{F}_{i2}$ **THEN**

$$\dot{\mathcal{X}}(t) = \bar{\mathcal{A}}_i\mathcal{X}(t) + \bar{\mathcal{B}}_i\mathcal{U}(t) \tag{5a}$$
$$\mathcal{Y}(t) = \bar{\mathcal{C}}_i\mathcal{X}(t) \tag{5b}$$

where $\mathcal{F}_{i1}$, $\mathcal{F}_{i2}$ are fuzzy sets, $\xi_1(t)$, $\xi_2(t)$ are premise variables, $\mathcal{Y}(t)$ is the measured output vector, $\bar{\mathcal{C}}_i$ is the output matrix, and

$$\bar{\mathcal{A}}_i = \begin{bmatrix} 0_{3\times3} & \mathcal{R}_i \\ \mathcal{B} & \mathcal{A} \end{bmatrix}, \bar{\mathcal{B}}_i = \bar{\mathcal{B}}$$
$$\mathcal{R}_1 = \begin{bmatrix} 1 & -1/2 & 0 \\ 1/2 & 1 & 0 \\ 0 & 0 & 1 \end{bmatrix}, \mathcal{R}_2 = \begin{bmatrix} \sqrt{3}/2 & -1/2 & 0 \\ 1/2 & \sqrt{3}/2 & 0 \\ 0 & 0 & 1 \end{bmatrix}$$
$$\mathcal{R}_3 = \begin{bmatrix} 1 & 1/2 & 0 \\ -1/2 & 1 & 0 \\ 0 & 0 & 1 \end{bmatrix}, \mathcal{R}_4 = \begin{bmatrix} \sqrt{3}/2 & 1/2 & 0 \\ -1/2 & \sqrt{3}/2 & 0 \\ 0 & 0 & 1 \end{bmatrix}$$

The nonlinear AUV model represented using T-S fuzzy rules is given by [1]:

$$\dot{\mathcal{X}}(t) = \sum_{i=1}^{4} \Gamma_i[\xi(t)][\bar{\mathcal{A}}_i\mathcal{X}(t) + \bar{\mathcal{B}}_i\mathcal{U}(t)] \tag{6a}$$
$$\mathcal{Y}(t) = \sum_{i=1}^{4} \Gamma_i[\xi(t)]\mathcal{C}_i\mathcal{X}(t) \tag{6b}$$

where

$$\Gamma_i[\xi(t)] = \frac{\lambda_i[\xi(t)]}{\sum_{j=1}^{4}\lambda_j[\xi(t)]}$$
$$\lambda_i[\xi_1(t)] = \mathcal{F}_{i1}[\xi_1(t)]\mathcal{F}_{i2}[\xi_2(t)], \lambda_i[\xi_1(t)] > 0$$
$$\sum_{i=1}^{4}\lambda_i[\mu(t)] = 1$$

and $\mathcal{F}_{i1}[\xi_1(t)]$ and $\mathcal{F}_{i1}[\xi_2(t)]$ have the same definitions as in [34].

III. DESIGN OF DELTA-SIGMA-BASED 1-BIT PID CONTROLLER

The schematic of a Delta-Sigma-based control system consists of an encoder ($\mathfrak{E}_{\Delta\Sigma}$), a decoder ($\mathfrak{D}_{\Delta\Sigma}$) and a communication channel as shown in Fig. 1. In the following, we briefly outline how these components operate before giving the comprehensive architecture of a **1**-bit PID controller based on Delta-Sigma principles.

A. ANALYSIS OF DELTA-SIGMA MODULATOR

Delta-Sigma modulator is one of the key components of the Delta-Sigma-based control system. It consists of two major components, i.e. a Delta-Sigma encoder $\mathfrak{E}_{\Delta\Sigma}$ and a Delta-Sigma decoder $\mathfrak{D}_{\Delta\Sigma}$, which are connected to each other through a communication channel as shown in Fig. 2 [35], [36].

In Fig. 2, the dotted lines represent the signals that are sent through the communication channel. Each encoder $\mathfrak{E}_{\Delta\Sigma}$ comprises of a 2-level quantiser, a multiplexer and an integrator. This multiplexer encodes the $\hat{\mu}(t)$ into a bit stream signal $\hat{\chi}(t)$. To reconstruct the signal $\hat{\chi}(t)$, each decoder $\mathfrak{D}_{\Delta\Sigma}$ comprise of a low pass filter and a multiplexer.

It is essential to understand the conditions in which the quantised signal ($\tilde{\mu}(t)$) is equal to the original signal ($\hat{\mu}(t)$) before discussing further principles of the Delta-Sigma-based **1**-bit PID controller. It is shown that $\tilde{\mu}(t)$ resembles $\hat{\mu}(t)$ if the input to the 2-level quantiser is less than the gain of the quantiser [11], [31].

Let us consider a continuous-time Delta-Sigma modulator which has $\mathcal{P}$ number of input channels [31]. Then,

$$\dot{\mathcal{S}}(t) = \hat{\mu}(t) - \tilde{\mu}(t) \tag{7}$$
$$\tilde{\mu}(t) = \mathcal{Q} \cdot sgn(\mathcal{S}(t)) \tag{8}$$

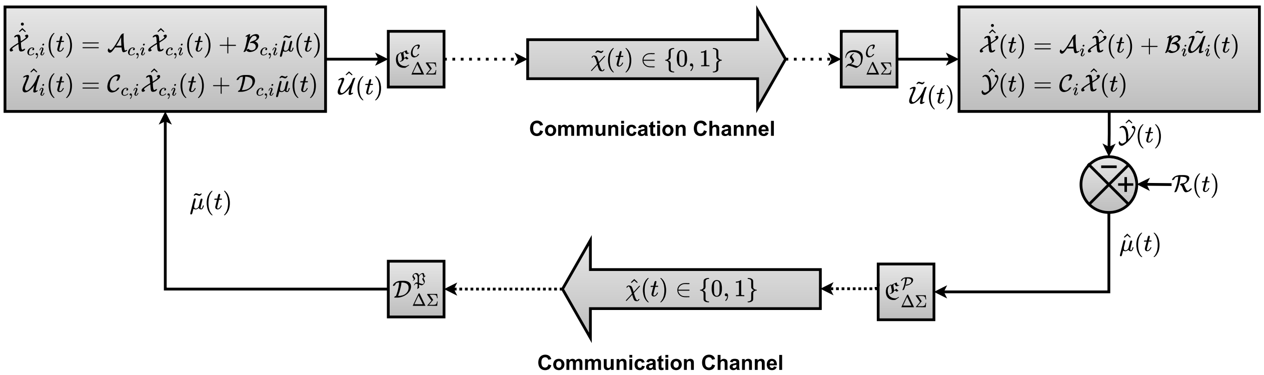

FIGURE 1. Delta-Sigma-based control system.

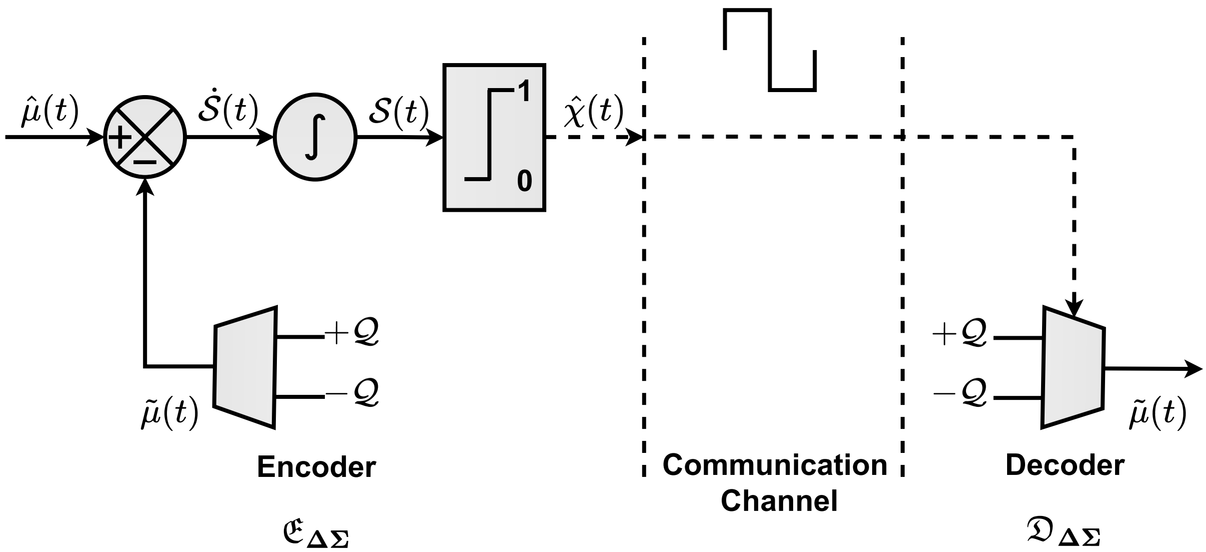

FIGURE 2. Delta-Sigma modulator.

where $\mathcal{Q} \in \mathrm{R}^{\mathcal{P}\times\mathcal{P}}$ is the gain of the 2-level quantiser, $\tilde{\mu}(t) \in \mathrm{R}^{\mathcal{P}}$ is the output of the decoder $\mathfrak{D}^x_{\Delta\Sigma}$ and $\hat{\mu}(t) \in \mathrm{R}^{\mathcal{P}}$ is the input to the encoder $\mathfrak{E}^x_{\Delta\Sigma}$.

Remark 1: To ensure that the sliding mode exist such that $\mathcal{S}^T\dot{\mathcal{S}} < 0$, the gain of the 2-level quantiser must be selected such that:

$$\left\|\hat{\mu}(t)\right\| \leq \lambda_{max}(\mathcal{Q}) \tag{9}$$

where λ_{max} denotes the largest eigenvalue of the 2-level quantiser gain $\mathcal{Q}$ [27].

In order for the Delta-Sigma modulator to be in the sliding surface, the following two conditions must be satisfied [27]:

$$\dot{\mathcal{S}} = 0$$
$$\tilde{\mu}(t) \equiv \hat{\mu}(t)$$

In order for the Delta-Sigma modulator to be in the sliding surface, the following two conditions must be satisfied [27]:

$$\dot{\mathcal{S}} = 0$$
$$\tilde{\mu}(t) \equiv \hat{\mu}(t)$$

This is often known as the equivalent control and can be expressed as [27]:

$$\hat{\mu}(t)_{(eq)} \equiv \mathcal{Q}\sigma(t) \tag{10}$$

where

$$\begin{aligned}\sigma(t) &= [sgn(\mathcal{S}(t))]_{av}\\ &= sgn(\mathcal{S}(t)) - \alpha\dot{\sigma}(t), \quad \in [-1, 1]\end{aligned}$$

and α denotes the low-pass filter time-constant of $\mathfrak{D}^x_{\Delta\Sigma}$.

B. DYNAMICS OF DELTA-SIGMA MODULATOR BASED CONTROL SYSTEM

The design of the Delta-Sigma-based **1**-bit controller is executed assuming that the system is linear. Note that this is not a limitation of this controller because if the system is nonlinear, it can be represented by multiple linear subsystems using T-S fuzzy modelling. In this study, the nonlinear plant in (1), is represented by multiple linear subsystems as described in (6). Let the fuzzy i^{th} linear subsystem be represented as:

$$\dot{\mathcal{X}}(t) = \mathcal{A}_i\mathcal{X}(t) + \mathcal{B}_i\mathcal{U}_i(t)$$
$$\mathcal{Y}(t) = \mathcal{C}_i\mathcal{X}(t) \tag{11}$$

where $\mathcal{X}(t) \in \mathbb{R}^{\mathcal{N}}$ are the states of the nonlinear plant, $\mathcal{U}_i(t) \in \mathbb{R}^{\mathcal{M}}$ are the inputs or the control signals of the local controller of the i^{th} AUV subsystem, and $\mathcal{Y}_i(t) \in \mathbb{R}^{\mathcal{P}}$ are the outputs of the nonlinear plant.

To stabilise i^{th} of the AUV subsystem described in (11), a local linear controller is designed and is described as:

$$\dot{\mathcal{X}}_{c,i}(t) = \mathcal{A}_{c,i}\mathcal{X}_{c,i}(t) + \mathcal{B}_{c,i}\mu(t)$$
$$\mathcal{U}_i(t) = \mathcal{C}_{c,i}\mathcal{X}_{c,i}(t) + \mathcal{D}_{c,i}\mu(t) \tag{12}$$

where $\mathcal{X}_{c,i}(t) \in \mathbb{R}^{\mathcal{L}}$ denotes the local controller states and $\mu(t) \in \mathbb{R}^{\mathcal{P}}$ represents the error signals. Note that the control design procedure is generic and applicable to any existing linear feedback controllers. Without loss of generality, it is first assumed for the reference signal $\mathcal{R}(t) = 0$, hence $\mu(t) = -\mathcal{Y}(t)$ (see remark 2 when $\mathcal{R}(t) \neq 0$)). Combining the i^{th} AUV subsystem dynamics (11) and controller dynamics in (12), the closed loop dynamics of i^{th} AUV subsystem is expressed as:

$$\dot{\mathcal{X}}_{cl,i}(t) = \mathcal{A}_{cl,i}\mathcal{X}_{cl,i}(t) \tag{13}$$

where

$$\mathcal{X}_{cl,i}(t) = \begin{bmatrix} \mathcal{X}(t) \\ \mathcal{X}_{c,i}(t) \end{bmatrix},$$
$$\mathcal{A}_{cl,i} = \begin{bmatrix} \mathcal{A}_i - \mathcal{B}_i\mathcal{D}_{c,i}\mathcal{C}_i & \mathcal{B}_i\mathcal{C}_{c,i} \\ -\mathcal{B}_{c,i}\mathcal{C}_i & \mathcal{A}_{c,i} \end{bmatrix}$$

It is worth noting that since the controller (12) is designed to stabilised the i^{th} AUV subsystem under parallel distributed compensation, all eigenvalues of $\mathcal{A}_{cl,i}$ must be negative. Fig. 1 shows the schematic of the Delta-Sigma-based control system where the $\mathfrak{E}_{\Delta\Sigma}$ and $\mathfrak{D}_{\Delta\Sigma}$ are inserted. These two elements work as encoder and decoder at the transmitter and the receiver. $\mathfrak{E}_{\Delta\Sigma}$ encodes the $\hat{\mu}$ signal into a bit-stream signal at the transmitter and $\mathfrak{D}_{\Delta\Sigma}$ decodes the bit-stream signal that is received through the communication channel in to $\tilde{\mu}$. As mentioned before for a AUV subsystem with $\mathcal{P}$ outputs, we require $\mathcal{P}$ number of encoders and decoders.

In the following, we illustrate the mathematical relationship between the output of the $\mathfrak{D}_{\Delta\Sigma}$ and the input of the $\mathfrak{E}_{\Delta\Sigma}$ as:

$$\tilde{\mu}(t) = \text{diag}\left\{\mathfrak{E}_{\Delta\Sigma_j} \circ \mathfrak{D}_{\Delta\Sigma_j}\right\} * \hat{\mu}(t) = \mathcal{Q}\ \text{sgn}(\mathcal{S}(t)) \tag{14}$$

where

$$\dot{\mathcal{S}}(t) = \hat{\mu}(t) - \tilde{\mu}(t) = \hat{\mu}(t) - \mathcal{Q}\ \text{sgn}(\mathcal{S}(t))$$
$$= -\hat{\mathcal{Y}}(t) - \mathcal{Q}\ \text{sgn}(\mathcal{S}(t)),\ (\because\ \mathcal{R}(t) = 0) \tag{15}$$

where $\mathcal{Q} \in \mathbb{R}^{\mathcal{P}\times\mathcal{P}}$. Under ideal conditions, the input of the $\mathfrak{E}_{\Delta\Sigma}$ and the output of the $\mathfrak{D}_{\Delta\Sigma}$ are equal ($\tilde{\mu}(t) = \hat{\mu}(t)$).

The signals $\mathcal{X}(t)$, $\mathcal{U}_i(t)$, $\mathcal{X}_{c,i}(t)$, $\mathcal{Y}(t)$ and $\mu(t)$ of typical control system, which are described in (11) and (12), are replaced by $\hat{\mathcal{X}}(t)$, $\hat{\mathcal{U}}_i(t)$, $\hat{\mathcal{X}}_{c,i}(t)$, $\hat{\mathcal{Y}}(t)$ and $\tilde{\mu}(t)$, respectively for Delta-Sigma-based control system.

The dynamics of the closed loop control system based on Delta-Sigma-based **1**-bit controller, for the i^{th} AUV subsystem, is expressed as:

$$\begin{bmatrix} \dot{\hat{\mathcal{X}}}_{cl,i}(t) \\ \dot{\mathcal{S}}(t) \end{bmatrix} = \begin{bmatrix} \mathcal{A}_{1,i} & \mathbf{0} \\ \mathcal{A}_{2,i} & \mathbf{0} \end{bmatrix} \begin{bmatrix} \hat{\mathcal{X}}_{cl,i}(t) \\ \mathcal{S}(t) \end{bmatrix} + \begin{bmatrix} \mathcal{B}_{1,i} \\ \mathcal{B}_{2,i} \end{bmatrix} \tilde{\mu}(t) \tag{16}$$

where $\hat{\mathcal{X}}_{cl,i}(t) = [\hat{\mathcal{X}}(t) \quad \hat{\mathcal{X}}_{c,i}(t)]^T$ and

$$\mathcal{A}_{1,i} := \begin{bmatrix} \mathcal{A}_i & \mathcal{B}_i\mathcal{B}_{c,i} \\ \mathbf{0} & \mathcal{A}_{c,i} \end{bmatrix}, \quad \mathcal{B}_{1,i} := \begin{bmatrix} \mathcal{B}_i\mathcal{D}_{c,i} \\ \mathcal{B}_{c,i} \end{bmatrix}$$
$$\mathcal{A}_{2,i} := [-\mathcal{C}_i \quad \mathbf{0}], \quad \mathcal{B}_{2,i} := -I_{\mathcal{P}} \tag{17}$$

with $\mathcal{A}_{1,i} \in \mathbb{R}^{(\mathcal{N}+\mathcal{L})\times(\mathcal{N}+\mathcal{L})}$, $\mathcal{A}_{2,i} \in \mathbb{R}^{\mathcal{P}\times(\mathcal{N}+\mathcal{V})}$ $\mathcal{B}_{1,i} \in \mathbb{R}^{(\mathcal{N}+\mathcal{L})\times\mathcal{P}}$ and $\mathcal{B}_{2,i} \in \mathbb{R}^{\mathcal{P}\times\mathcal{P}}$.

C. STABILITY ANALYSIS OF DELTA-SIGMA MODULATOR BASED CONTROL SYSTEM

The following section derives the stability conditions for the Delta-Sigma-based **1**-bit control system in (16), where $\mathcal{X}(t)$ and $\mathcal{X}_{cl,i}(t)$ denote the states of the open and closed loop system (without the Delta-Sigma modulator), respectively. $\hat{\mathcal{X}}(t)$ and $\hat{\mathcal{X}}_{cl,i}(t)$ represent the corresponding states of Delta-Sigma modulator based control system.

Assumption 1: The classical feedback control system described in (13) is stable ($\mathcal{A}_{cl,i}$ is Hurwitz).

In order to establish the stability conditions of the Delta-Sigma modulator based control system for the i^{th} AUV subsystem, it is shown that $\hat{\mathcal{X}}_{cl,i}(t) \to \mathcal{X}_{cl,i}(t)$. This implicitly suggest that the Delta-Sigma modulator based control system maintain the stability properties of the classical feedback system.

Theorem 1: If there exists a positive-definite symmetric matrix $\mathcal{Q}$ such that

$$\left\|\hat{\mathcal{X}}_{cl,i}(t)\right\| \leq \lambda_{min}(\mathcal{Q}) / \|\mathcal{C}_i\|, \tag{18}$$

for all $i = 1, 2, 3, 4$, then the state trajectories of the AUV system are driven towards the sliding manifold.

Proof: Consider a Lyapunov function as:

$$\Lambda(t) = \frac{1}{2}\mathcal{S}^T(t)\mathcal{S}(t) \tag{19}$$

where $\dot{\mathcal{S}}(t) = -\hat{\mathcal{Y}}(t) - \mathcal{Q}\ \text{sgn}(\mathcal{S}(t))$ (from (15)).

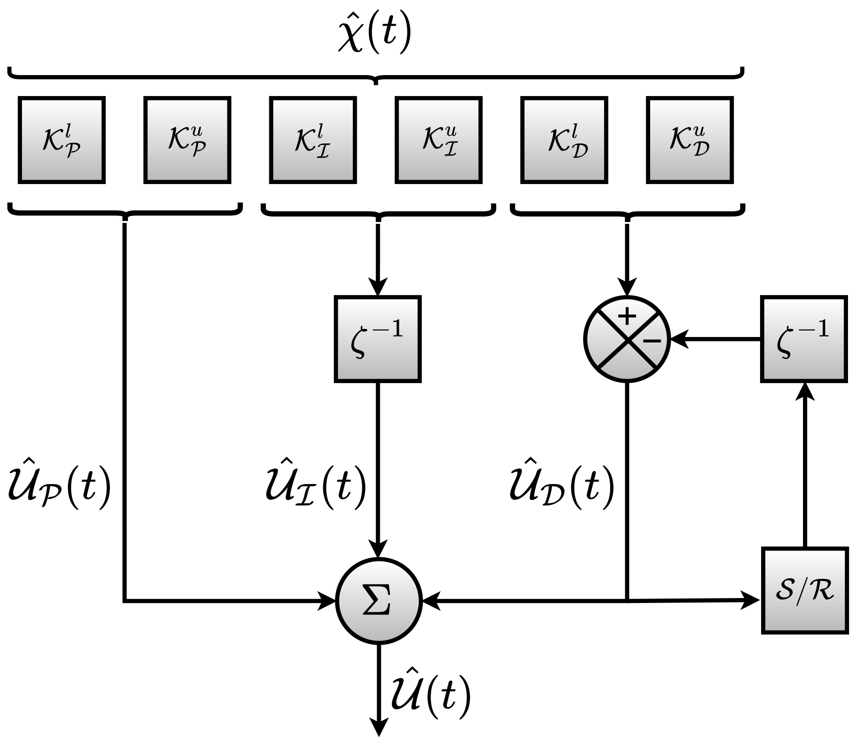

FIGURE 3. Delta-Sigma-based 1-bit PID controller.

By differentiating $\Lambda(\mathrm{t})$ gives,

$$\begin{aligned}
\dot{\Lambda}(\mathrm{t}) &= \frac{1}{2}(\mathcal{S}^T(\mathrm{t})\dot{\mathcal{S}}(\mathrm{t}) + \dot{\mathcal{S}}^T(\mathrm{t})\mathcal{S}(\mathrm{t})) \\
&= \frac{1}{2}\{\mathcal{S}^T(\mathrm{t})(-\hat{\mathcal{Y}}(\mathrm{t}) - \mathcal{Q}sgn(\mathcal{S}(\mathrm{t})))\} \\
&\quad + \frac{1}{2}\{(-\hat{\mathcal{Y}}(\mathrm{t}) - \mathcal{Q}sgn(\mathcal{S}(\mathrm{t})))^T\mathcal{S}(\mathrm{t})\} \\
&= \frac{1}{2}\{\mathcal{S}^T(\mathrm{t})(-\mathcal{C}_i\hat{\mathcal{X}}(\mathrm{t}) - \mathcal{Q}sgn(\mathcal{S}(\mathrm{t})))\} \\
&\quad + \frac{1}{2}\{(-\mathcal{C}_i\hat{\mathcal{X}}(\mathrm{t}) - \mathcal{Q}sgn(\mathcal{S}(\mathrm{t})))^T\mathcal{S}(\mathrm{t})\} \\
&= -\frac{1}{2}\{(\mathcal{S}^T(\mathrm{t})\mathcal{C}\hat{\mathcal{X}}(\mathrm{t}) + \hat{\mathcal{X}}^T(\mathrm{t})\mathcal{C}_i^T\mathcal{S}(\mathrm{t}))\} \\
&\quad + \frac{1}{2}\{(\mathcal{S}^T(\mathrm{t})\mathcal{Q}sgn(\mathcal{S}(\mathrm{t}))) + (\mathcal{Q}sgn(\mathcal{S}(\mathrm{t})))^T\mathcal{S}(\mathrm{t})\} \\
&= -\frac{1}{2}\{(\mathcal{S}^T(\mathrm{t})\mathcal{C}_i\hat{\mathcal{X}}(\mathrm{t}) + \hat{\mathcal{X}}^T(\mathrm{t})\mathcal{C}_i^T\mathcal{S}(\mathrm{t}))\} \\
&\quad + \frac{1}{2}\{(2\mathcal{S}^T(\mathrm{t})\mathcal{Q}sgn(\mathcal{S}(\mathrm{t})))\} \\
&\leq -\frac{1}{2}(\mathcal{S}^T(\mathrm{t})\mathcal{C}_i\hat{\mathcal{X}}(\mathrm{t}) + \hat{\mathcal{X}}^T\mathcal{C}_i^T\mathcal{S}(\mathrm{t})) \\
&\quad - \frac{1}{2}(\mathcal{S}^T(\mathrm{t})\lambda_{min,i}(\mathcal{Q}_i)I_{\mathcal{P}} \cdot sgn(\mathcal{S}(\mathrm{t})) \\
&\leq -\|\mathcal{S}(\mathrm{t})\|\,(\lambda_{min}(\mathcal{Q}) - \|\mathcal{C}_i\|\,\left\|\hat{\mathcal{X}}(\mathrm{t})\right\|). \qquad (20)
\end{aligned}$$

If the quantiser gain $\mathcal{Q}$ of the Delta-Sigma modulator is chosen such that $\left\|\hat{\mathcal{X}}(\mathrm{t})\right\| \leq \lambda_{min}(\mathcal{Q})/\|\mathcal{C}_i\|$, for all $i = 1, 2, 3, 4$, then $\dot{\Lambda}(\mathrm{t}) < 0$, which ensures that the state trajectories of the Delta-Sigma control system for the AUV system, are steered towards the sliding manifold [11], [31]. ∎

Remark 2: Consider the case where $\mathcal{R}(\mathrm{t}) \neq 0$, by following a similar procedure described in Theorem 1, it can easily be proved that $\dot{\Lambda}(\mathrm{t}) \leq -\|\mathcal{S}(\mathrm{t})\|\,(\lambda_{min}(\mathcal{Q}) - \eta)$ where $\eta = \|\mathcal{R}(\mathrm{t})\| + \|\mathcal{C}_i\|\,\left\|\hat{\mathcal{X}}(\mathrm{t})\right\|$.

Theorem 2: If for all $i = 1, 2, 3, 4$, $\left\|\hat{\mathcal{X}}_{cl,i}(\mathrm{t})\right\| \leq \lambda_{min}(\mathbf{Q})/\|\mathcal{C}_i\|$ then, under ideal sliding condition $\hat{\mathcal{X}}_{cl,i}(\mathrm{t}) \equiv \mathcal{X}_{cl,i}(\mathrm{t})$.

Proof: It can be shown from (14) that:

$$\dot{\hat{\mathcal{X}}}_{cl,i}(\mathrm{t}) = \mathcal{A}_{1,i}\hat{\mathcal{X}}_{cl,i}(\mathrm{t}) + \mathcal{B}_{1,i}\tilde{\mu}_{eq}(\mathrm{t}) \qquad (21)$$

$$\dot{\mathcal{S}}(\mathrm{t}) = \mathcal{A}_{2,i}\hat{\mathcal{X}}_{cl,i}(\mathrm{t}) + \mathcal{B}_{2,i}\tilde{\mu}_{eq}(\mathrm{t}) \qquad (22)$$

where $\tilde{\mu}_{eq}(\mathrm{t}) = \mathcal{Q}sgn(\mathcal{S}(\mathrm{t}))_{eq}$ (refer (16)) and $sgn(\mathcal{S}(\mathrm{t}))_{eq} \in (-1, 1)$.

From (22),

$$\tilde{\mu}_{eq}(\mathrm{t}) = \mathcal{B}_{2,i}^{-1}\dot{\mathcal{S}}(\mathrm{t}) - \mathcal{B}_{2,i}^{-1}\mathcal{A}_{2,i}\hat{\mathcal{X}}_{cl,i}(\mathrm{t}) \qquad (23)$$

Substituting $\tilde{\mu}_{eq}(t)$ from (23) into (21) and after simplifying using (16) gives,

$$\begin{aligned}\dot{\hat{\mathcal{X}}}_{cl,i}(t) &= \mathcal{A}_{1,i}\hat{\mathcal{X}}_{cl,i}(t) + \mathcal{B}_{1,i}\{\mathcal{B}_{2,i}^{-1}\dot{\mathcal{S}}(t) - \mathcal{B}_{2,i}^{-1}\mathcal{A}_{2,i}\hat{\mathcal{X}}_{cl,i}(t)\}\\ &= (\mathcal{A}_{1,i} - \mathcal{B}_{1,i}\mathcal{B}_{2,i}^{-1}\mathcal{A}_{2,i})\hat{\mathcal{X}}_{cl,i}(t) + \mathcal{B}_{1,i}\mathcal{B}_{2,i}^{-1}\dot{\mathcal{S}}(t)\\ &= \left(\begin{bmatrix}\mathcal{A}_i & \mathcal{B}_i\mathcal{C}_{c,i}\\ 0 & \mathcal{A}_{c,i}\end{bmatrix} + \begin{bmatrix}\mathcal{B}_i\mathcal{D}_{c,i}\\ \mathcal{B}_{c,i}\end{bmatrix}\begin{bmatrix}-\mathcal{C}_i & 0\end{bmatrix}\right)\hat{\mathcal{X}}_{cl,i}(t) \quad (24)\\ &\quad + \mathcal{B}_{1,i}\mathcal{B}_{2,i}^{-1}\dot{\mathcal{S}}(t)\\ &= \mathcal{A}_{cl,i}\hat{\mathcal{X}}_{cl,i}(t) + \mathcal{B}_{1,i}\mathcal{B}_{2,i}^{-1}\dot{\mathcal{S}}(t) \quad (25)\end{aligned}$$

From (13) and (24), it can easily be observed that as $\dot{\mathcal{S}}(t) \to 0$, the state trajectories $\hat{\mathcal{X}}_{cl,i}(t) \to \mathcal{X}_{cl,i}(t)$. ∎

Lemma 1: [27] To avoid the system being unstable during the sliding mode phase, the initial conditions of the switching function $\mathcal{S}_k(t_0)$ is selected such that:

$$|\mathcal{S}_k(t_0)| \leq \lambda_{min}(\mathcal{Q})\ \forall k \in \{1, 2, \ldots, \mathcal{P}\} \quad (26)$$

Remark 3: To relax the assumption of infinite sampling, a boundary layer can be introduced. Note that sliding mode takes place in this boundary layer $\mathfrak{S}_i$ where:

$$\|\mathfrak{S}_i\| \leq \|\mathcal{C}_i\|. \quad (27)$$

Remark 4: Note that if the controlled plant is nonlinear and if the system dynamics are represented by a set of T-S fuzzy rules, T-S fuzzy PID controllers can be designed for each subsystem of the T-S fuzzy model using linear control theory. Then using parallel distributed compensation (PDC), T-S fuzzy PID controller can be designed for the whole nonlinear system.

D. SELECTION OF PID TUNING PARAMETERS

The stability conditions for the Delta-Sigma modulator based **1**-bit control system was derived in the previous section. Although we derived the stability conditions considering the AUV subsystem, the controller design procedure is generic and various other controllers can be designed using this framework.

The schematic of the Delta-Sigma-based **1**-bit PID controller is depicted in Fig. 3. As a first step, for each linear subsystem, estimated PID gains are calculated following a similar procedure as described in [37]. In the next step, lower and upper bounds of the proportional gain $[\mathcal{K}_{\mathcal{P},i}^l, \mathcal{K}_{\mathcal{P},i}^u]$, integral gain $[\mathcal{K}_{\mathcal{I},i}^l, \mathcal{K}_{\mathcal{I},i}^u]$, differential gains $[\mathcal{K}_{\mathcal{D},i}^l, \mathcal{K}_{\mathcal{D},i}^u]$ are selected around those initially obtained values. *Shift registers* are used, instead of multipliers, to keep hardware consumption minimal. The output of the Delta-Sigma-based **1**-bit PID controller for the i^{th} AUV subsystem, is given by:

$$\hat{\mathcal{U}}_i(t) = \mathcal{K}_{P,i} + \frac{\mathcal{K}_{I,i}h}{\zeta(t)} + \frac{\mathcal{K}_{D,i}\mathcal{N}_{\mathcal{D},i}\tau}{\zeta(t) + \mathcal{N}_{\mathcal{N},i}\tau} \quad (28)$$

where the τ and $\mathcal{N}_{\mathcal{D},i}$ denote the sampling time and the filter coefficient of the differentiator. Furthermore:

$$\mathcal{N}_{\mathcal{D},i}\tau = 2^{-\mathcal{R}}, \quad \mathcal{R} \in \mathbb{N}_0 \quad (29)$$

$$\zeta(t) = \mathcal{X}(t+\tau) - \mathcal{X}(t) \quad (30)$$

After designing the Delta-Sigma-based **1**-bit PID controller, the focus shifts to design an output feedback controller for comparison purposes. This type of of controller has been chosen as reference, as it has been applied successfully in various applications. Additionally, it is of interest to investigate its robustness against various disturbances in underwater environment with limited communication bandwidth. Thus, we derive in the following an output feedback controller for AUV systems. The design procedure of the output feedback controller differs slightly from the output feedback controllers described in the literature. During the design, we have used results from [38] to reformulate the bi-linear problem in to a linear matrix inequality.

IV. DESIGN OF OUTPUT FEEDBACK CONTROLLER

In the following section, we describe the procedure for designing an output feedback controller for the AUV presented in section II.

Consider the nonlinear system described in (5). Define:

$$\bar{\mathcal{A}}(\lambda) = \sum_{i=1}^{4} \lambda_i[\xi(t)]\mathcal{A}_i$$

$$\bar{\mathcal{B}}(\lambda) = \sum_{i=1}^{4} \lambda_i[\xi(t)]\mathcal{B}_i$$

$$\bar{\mathcal{C}}(\lambda) = \sum_{i=1}^{4} \lambda_i[\xi(t)]\mathcal{C}_i \quad (31)$$

For the nonlinear plant described in (5), the fuzzy output feedback controller is defined as:

$$\mathcal{U}(t) = \bar{\mathcal{K}}(\lambda)\mathcal{Y}(t) \quad (32)$$

where,

$$\bar{\mathcal{K}}(\lambda) = \sum_{i=1}^{r} \lambda_i[\xi(t)]\mathcal{K}_i \quad (33)$$

Note that $\mathcal{K}_i, \quad i = 1, 2, 3, 4$ are the local controller gains which are to be designed. Integrating the output feedback fuzzy controller in (32) to the global AUV fuzzy plant in (6), the closed loop output feedback control system results to:

$$\dot{\mathcal{X}}(t) = \left(\bar{\mathcal{A}}(\lambda) + \bar{\mathcal{B}}(\lambda)\bar{\mathcal{K}}(\lambda)\bar{\mathcal{C}}(\lambda)\right)\mathcal{X}(t) \quad (34)$$

Note that following lemmas are necessary for the proof and are presented here for sake of completeness.

Lemma 2: [39] Denote the set $\mathfrak{T} = \{t\}$ and let $\mathfrak{H}(t)$, $\mathfrak{J}_1(t), \ldots, \mathfrak{J}_l(t)$ be some functional or functions. Further define domain $\mathfrak{H}$:

$$\mathfrak{H} = \{t \in \mathfrak{T} : \mathfrak{J}_1(t) \leq 0, \ldots, \mathfrak{J}_l(t) \leq 0\}. \quad (35)$$

If there exist $\kappa_1 \geq 0, \ldots, \kappa_l \geq 0$ such that

$$\mathfrak{H}(t) - \sum_{j=1}^{l} \kappa_j\mathfrak{J}_j(t) < 0, \quad (36)$$

then, $\mathfrak{H}(t) < 0\ \forall t \in \mathfrak{H}$.

Lemma 3: *[38] Consider a matrix $\mathfrak{M}$ of the form*

$$\mathfrak{M} = \begin{pmatrix} \mathfrak{A} & \mathfrak{B} \\ \mathfrak{B}^T & \mathfrak{C} \end{pmatrix},$$

then the following are true given that $\mathfrak{C}$ is invertible,

i. *If $\mathfrak{A} - \mathfrak{B}\mathfrak{C}^{-1}\mathfrak{B}^T > 0$ and $\mathfrak{C} > 0$, then $\mathfrak{M} > 0$*
ii. *If $\mathfrak{A} - \mathfrak{B}\mathfrak{C}^{-1}\mathfrak{B}^T \geq 0$ and $\mathfrak{C} > 0$, then $\mathfrak{M} \geq 0$.*

Lemma 4: *[38]*

i. *A matrix-valued mapping $\mathfrak{G}$ is positive semi-definite-convex on $\mathfrak{X}$ if and only if for any $\mathfrak{V} \in \mathbb{R}^{\mathfrak{P}}$, the function $\mathfrak{F} := \mathfrak{v}^T\mathfrak{G}(x)\mathfrak{v}$ is convex on $\mathfrak{X}$.*
ii. *A mapping $\mathfrak{G}$ is positive semi-definite-convex on $\mathfrak{X}$ if and only if for all $\mathfrak{x}$ and $\mathfrak{y}$ in $\mathfrak{X}$.*

$$\mathfrak{G}(\mathfrak{y}) - \mathfrak{G}(\mathfrak{x}) \geq \mathfrak{D}\mathfrak{G}(\mathfrak{x})(\mathfrak{y} - \mathfrak{x})$$

Theorem 3: *If there exists a symmetric matrix $\mathcal{P} > 0$ and matrices $\mathcal{K}_i$, $i = 1, 2, 3, 4$ that satisfy the following conditions:*

$$\begin{bmatrix} \mathcal{A}_i^T\mathcal{P} + \mathcal{P}\mathcal{A}_i & \mathcal{P}\mathcal{B}_i & \star^T \\ \mathcal{B}_i^T\mathcal{P} & -I & 0 \\ \mathcal{B}_i^T\mathcal{P} + \mathcal{K}_i\mathcal{C}_i & 0 & -I \end{bmatrix} < 0, \quad i = 1, 2, 3, 4; \tag{37}$$

$$\begin{bmatrix} \frac{1}{2}\begin{pmatrix} \mathcal{A}_i^T\mathcal{P} + \mathcal{P}\mathcal{A}_i \\ +\mathcal{A}_j^T\mathcal{P} + \mathcal{P}\mathcal{A}_j \end{pmatrix} & \frac{1}{2}\mathcal{P} & \star^T \\ \frac{1}{2}\mathcal{P} & -\frac{1}{2}\begin{pmatrix} \mathcal{B}_i\mathcal{B}_j^T \\ +\mathcal{B}_j\mathcal{B}_i^T \end{pmatrix} & 0 \\ \frac{1}{2}\begin{pmatrix} \mathcal{B}_i^T\mathcal{P} + \mathcal{K}_i\mathcal{C}_j \\ +\mathcal{B}_j^T\mathcal{P} + \mathcal{K}_j\mathcal{C}_i \end{pmatrix} & 0 & -I \end{bmatrix} < 0, \quad i > j; \tag{38}$$

then, the system (34) is asymptotically stable.

Proof: Choose the Lyapunov function candidate as:

$$\Lambda(\mathrm{t}) = \mathcal{X}^T(\mathrm{t})\mathcal{P}\mathcal{X}(\mathrm{t}).$$

The time derivative of the $\Lambda(\mathrm{t})$ is:

$$\begin{aligned} \dot{\Lambda}(\mathrm{t}) &= \dot{\mathcal{X}}^T(\mathrm{t})\mathcal{P}\mathcal{X}(\mathrm{t}) + \mathcal{X}^T(\mathrm{t})\mathcal{P}\dot{\mathcal{X}}(\mathrm{t}) \\ &= \mathcal{X}^T(\mathrm{t})\left\{\bar{\mathcal{A}}(\lambda) + \bar{\mathcal{B}}(\lambda)\bar{\mathcal{K}}(\lambda)\bar{\mathcal{C}}(\lambda)\right\}^T\mathcal{P}\mathcal{X}(\mathrm{t}) \\ &\quad + \mathcal{X}^T(\mathrm{t})\mathcal{P}\left\{\bar{\mathcal{A}}(\lambda) + \bar{\mathcal{B}}(\lambda)\bar{\mathcal{K}}(\lambda)\bar{\mathcal{C}}(\lambda)\right\}\mathcal{X}(\mathrm{t}) \\ &\leq \mathcal{X}^T(\mathrm{t})\left\{\left(\bar{\mathcal{A}}(\lambda) + \bar{\mathcal{B}}(\lambda)\bar{\mathcal{K}}(\lambda)\bar{\mathcal{C}}(\lambda)\right)^T\mathcal{P}\right\}\mathcal{X}(\mathrm{t}) \\ &\quad + \mathcal{X}^T(\mathrm{t})\mathcal{P}\left\{\left(\bar{\mathcal{A}}(\lambda) + \bar{\mathcal{B}}(\lambda)\bar{\mathcal{K}}(\lambda)\bar{\mathcal{C}}(\lambda)\right)\right\}\mathcal{X}(\mathrm{t}) \\ &\quad + \mathcal{X}^T(\mathrm{t})\left\{\left(\bar{\mathcal{C}}(\lambda)^T\bar{\mathcal{K}}(\lambda)^T\bar{\mathcal{K}}(\lambda)\bar{\mathcal{C}}(\lambda)\right)\right\}\mathcal{X}(\mathrm{t}) \\ &= \mathcal{X}^T(\mathrm{t})\left\{\Psi_1 + \Psi_2^T\Psi_2\right\}\mathcal{X}(\mathrm{t}) \end{aligned} \tag{39}$$

where

$$\begin{aligned} \Psi_1 &= \mathcal{A}(\lambda)^T\mathcal{P} + \mathcal{P}\bar{\mathcal{A}}(\lambda) - \mathcal{P}\bar{\mathcal{B}}(\lambda)\bar{\mathcal{B}}(\lambda)^T\mathcal{P} \\ \Psi_2 &= \bar{\mathcal{B}}(\lambda)^T\mathcal{P} + \bar{\mathcal{K}}(\lambda)\bar{\mathcal{C}}(\lambda) \end{aligned}$$

From (39) it is clear that if:

$$\begin{aligned} \Psi &= \Psi_1 + \Psi_2^T\Psi_2 < 0 \\ \Psi &= \bar{\mathcal{A}}(\lambda)^T\mathcal{P} + \mathcal{P}\bar{\mathcal{A}}(\lambda) - \mathcal{P}\bar{\mathcal{B}}(\lambda)\bar{\mathcal{B}}(\lambda)^T\mathcal{P} \\ &\quad + \left(\bar{\mathcal{B}}(\lambda)^T\mathcal{P} + \bar{\mathcal{K}}(\lambda)\bar{\mathcal{C}}(\lambda)\right)^T \\ &\quad \times \left(\bar{\mathcal{B}}(\lambda)^T\mathcal{P} + \bar{\mathcal{K}}(\lambda)\bar{\mathcal{C}}(\lambda)\right) < 0, \end{aligned} \tag{40}$$

then the fuzzy system (34) is stable.

Using 3 and 4, we can express Ψ as:

$$\begin{aligned} \Psi &= \begin{bmatrix} \bar{\mathcal{A}}(\lambda)^T\mathcal{P} + \mathcal{P}\bar{\mathcal{A}}(\lambda) - \mathcal{P}\bar{\mathcal{B}}(\lambda)\bar{\mathcal{B}}(\lambda)^T\mathcal{P} & \star^T \\ \bar{\mathcal{B}}(\lambda)^T\mathcal{P} + \bar{\mathcal{K}}(\lambda)\bar{\mathcal{C}}(\lambda) & -I \end{bmatrix} \\ &= \sum_{i=1}^{4}\lambda_i\sum_{j=1}^{4}\lambda_j\begin{bmatrix} \bar{\mathcal{A}}(\lambda)^T\mathcal{P} + \mathcal{P}\bar{\mathcal{A}}(\lambda) - \mathcal{P}\bar{\mathcal{B}}(\lambda)\bar{\mathcal{B}}(\lambda)^T\mathcal{P} & \star^T \\ \bar{\mathcal{B}}(\lambda)^T\mathcal{P} + \bar{\mathcal{K}}(\lambda)\bar{\mathcal{C}}(\lambda) & -I \end{bmatrix} \\ &= \sum_{i=1}^{4}\lambda_i^2\begin{bmatrix} \mathcal{A}_i^T\mathcal{P} + \mathcal{P}\mathcal{A}_i - \mathcal{P}\mathcal{B}_i\mathcal{B}_i^T\mathcal{P} & \star^T \\ \mathcal{B}_i^T\mathcal{P} + \mathcal{K}_i\mathcal{C}_i & -I \end{bmatrix} \\ &\quad + \sum_{i<j}^{4}\lambda_i\lambda_j\begin{bmatrix} \frac{1}{2}\begin{pmatrix} \mathcal{A}_i^T\mathcal{P} + \mathcal{P}\mathcal{A}_i - \mathcal{P}\mathcal{B}_i\mathcal{B}_j^T\mathcal{P} \\ +\mathcal{A}_j^T\mathcal{P} + \mathcal{P}\mathcal{A}_j - \mathcal{P}\mathcal{B}_j\mathcal{B}_i^T\mathcal{P} \end{pmatrix} & \star^T \\ \frac{1}{2}\left(\mathcal{B}_i^T\mathcal{P} + \mathcal{K}_i\mathcal{C}_j + \mathcal{B}_j^T\mathcal{P} + \mathcal{K}_j\mathcal{C}_i\right) & -I \end{bmatrix} \\ &= \sum_{i=1}^{4}\lambda_i^2\begin{bmatrix} \mathcal{A}_i^T\mathcal{P} + \mathcal{P}\mathcal{A}_i & \mathcal{P}\mathcal{B}_i & \star^T \\ \mathcal{B}_i^T\mathcal{P} & -I & 0 \\ \mathcal{B}_i^T\mathcal{P} + \mathcal{K}_i\mathcal{C}_i & 0 & -I \end{bmatrix} \\ &\quad + \sum_{i<j}^{4}\lambda_i\lambda_j\begin{bmatrix} \frac{1}{2}\begin{pmatrix} \mathcal{A}_i^T\mathcal{P} + \mathcal{P}\mathcal{A}_i \\ +\mathcal{A}_j^T\mathcal{P} + \mathcal{P}\mathcal{A}_j \end{pmatrix} & \frac{1}{2}\mathcal{P} & \star^T \\ \frac{1}{2}\mathcal{P} & -\frac{1}{2}\begin{pmatrix} \mathcal{B}_i\mathcal{B}_j^T \\ +\mathcal{B}_j\mathcal{B}_i^T \end{pmatrix} & 0 \\ \frac{1}{2}\begin{pmatrix} \mathcal{B}_i^T\mathcal{P} + \mathcal{K}_i\mathcal{C}_j \\ +\mathcal{B}_j^T\mathcal{P} + \mathcal{K}_j\mathcal{C}_i \end{pmatrix} & 0 & -I \end{bmatrix} \end{aligned} \tag{41}$$

Thus, if (41) is less than zero, i.e. $\Psi < 0$, then the fuzzy system is stable (using Lemma 2). ∎

V. SIMULATION RESULTS

The robust capability of the proposed Delta-Sigma-based **1**-bit PID controller is investigated in a networked system and its performance was compared with an output feedback controller. The considered example is a nonlinear AUV system, which is represented by T-S fuzzy model consisting of 4-number of linear subsystems.

The block diagram of the employed network control system is shown in Fig. 4 and in Fig. 5. Following the common practice, it is assumed that the communication channel exists only in one side of the networked system. There, the control signal from the proposed Delta-Sigma **1**-bit PID controller or the output feedback controller is transmitted through a wireless communication channel to the AUV (in Fig. 1, $\hat{\mu}(\mathrm{t}) \equiv \tilde{\mu}(\mathrm{t})$). From Fig. 5, it can be observed that the wireless communication channel is implemented using

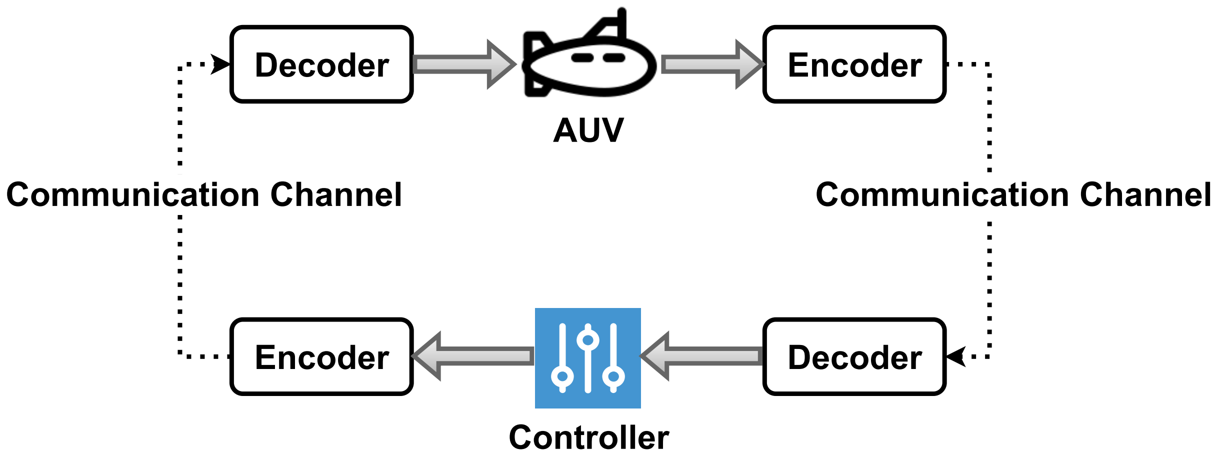

FIGURE 4. Networked control system.

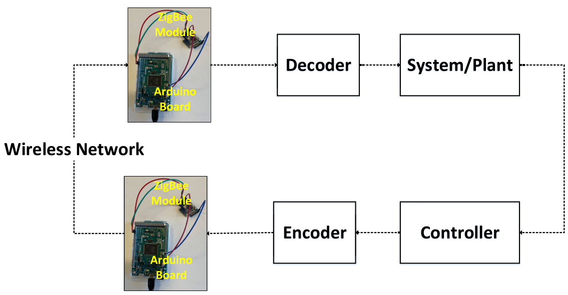

FIGURE 5. Networked control using ZigBee protocol based communication network.

two Arduino boards and two Zigbee modules as hardware in loop (HIL). The modulated signal is transmitted to the Zigbee module 2 in Arduino board 2 from the Zigbee module 1 in Arduino board 1. This board is connected to the computer and with the plant, the controller, and the quantiser. The Zigbee module 2 in Arduino board 2 acts as a hop device in another computer which transmits the signal back to the Zigbee module 1 in Arduino board 1 which then transmits the signal into the demodulator.

The nonlinear dynamics of AUV is described by (1) where [1]:

$$\mathcal{M} = \begin{bmatrix} 1.0852 & 0 & 0 \\ 0 & 2.0575 & -0.4087 \\ 0 & -0.4087 & 0.2153 \end{bmatrix}$$
$$\mathcal{N} = \begin{bmatrix} 0.0865 & 0 & 0 \\ 0 & 0.0762 & 0.1510 \\ 0 & 0.1510 & 0.0031 \end{bmatrix}$$
$$\mathcal{G} = \begin{bmatrix} 0.0389 & 0 & 0 \\ 0 & 0.0266 & 0 \\ 0 & 0 & 0 \end{bmatrix} \quad (42)$$

The various matrices described in (3) are:

$$\mathcal{A} = \begin{bmatrix} -0.0797 & 0 & 0 \\ 0 & -0.0818 & -0.1224 \\ 0 & -0.2254 & -0.2468 \end{bmatrix}$$
$$\mathcal{B} = \begin{bmatrix} -0.0358 & 0 & 0 \\ 0 & -0.0208 & 0 \\ 0 & -0.0394 & 0 \end{bmatrix}$$
$$\mathcal{D} = \begin{bmatrix} 0.9215 & 0 & 0 \\ 0 & 0.7802 & 1.4811 \\ 0 & 1.4811 & 7.4562 \end{bmatrix} \quad (43)$$

During the simulations it is assumed that the output matrices $\mathcal{C}_i = I_{3\times3} \quad i = 1, 2, 3, 4$ (see (5)). To emulate practical underwater environment, simulations are conducted considering a transmission delay of 0.01 seconds [40]. The gains of the output-feedback controller and the Delta-Sigma-based **1**-bit PID controller are designed following the procedures described in section-IV and section-III. In this simulation, the initial conditions of the surge velocity, sway velocity and yaw velocity is assumed to be 0.05, 0.01 and −0.01, respectively.

Initially, the effects of disturbances are not taken into consideration and the velocity response of the AUV were obtained without the controllers. The responses, depicted in Fig. 6, indicate that with the absence of the controllers, the AUV becomes unstable even with the absence of any disturbances such as currents.

Next, both the Delta-Sigma-based **1**-bit PID controller and the output-feedback controller are implemented without considering the effects of disturbances. The velocity responses of these controllers are shown in Fig. 7 and Fig. 8, respectively.

It can be seen from the results that both the controllers could stabilise the AUV system and return to the steady-state within practically acceptable times. However, the **1**-bit controller shows a high overshoot compared to the output feedback controller for the sway and yaw velocities. This is expected as the Delta-Sigma-based **1**-bit PID controller

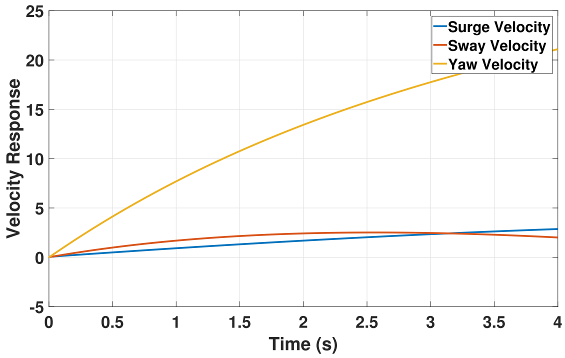

FIGURE 6. Velocity response of AUV without controllers.

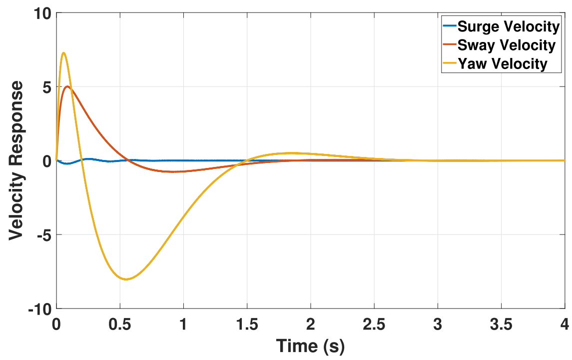

FIGURE 7. Velocity response of AUV with the Delta-Sigma-based 1-bit PID controller without disturbances.

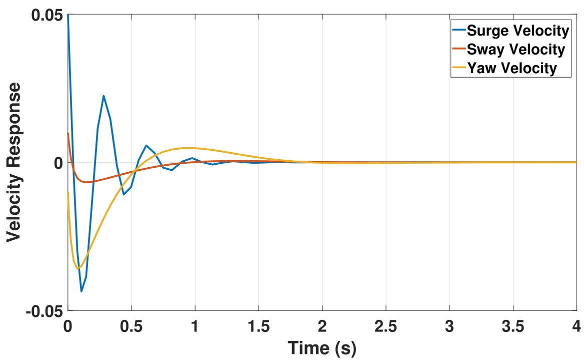

FIGURE 8. Velocity response of AUV with output-feedback controller without disturbances.

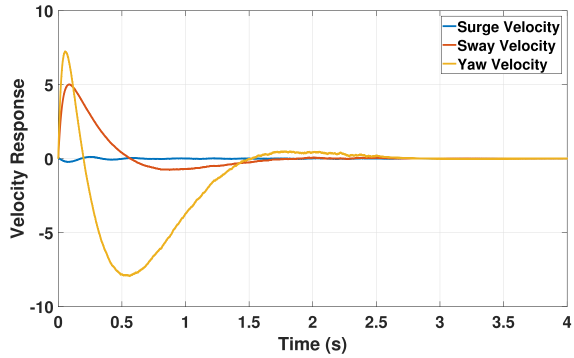

FIGURE 9. Velocity response of AUV with the Delta-Sigma-based 1-bit PID controller under moderate disturbances.

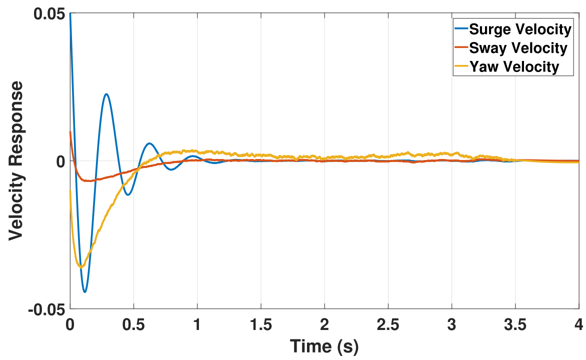

FIGURE 10. Velocity response of AUV with output-feedback controller under moderate disturbances.

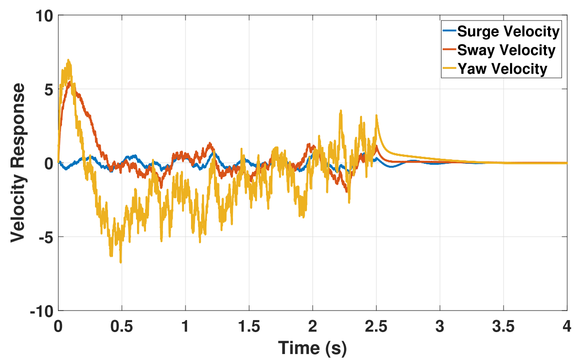

FIGURE 11. Velocity response of AUV with the Delta-Sigma-based 1-bit PID controller under extreme disturbances and limited network resources.

transmits **1**-bit as control signals to control the AUV unlike the output feedback controller which sends higher bit signals (e.g. 32-bit).

In the third phase, the effects of moderate disturbances, e.g. water currents, on the AUV system are considered. During simulations, the effects of these disturbances are reflected as measurement noise. The performance of the controllers are depicted in Fig. 9 and Fig. 10. Although, both these controllers results in stable dynamics, the performance of **1**-bit controllers is similar to the results shown in Fig. 7. However, the yaw velocity response of the output feedback controller takes longer time to reach the steady-state.

In the last phase, the robustness of these controllers are investigated further, where we consider the effects of extreme disturbances and *congestion attack*). These are incorporated into the simulation as measurement noise and packet losses, respectively. The resulting velocity response of the AUV with Delta-Sigma-based **1**-bit PID controller is shown in Fig. 11. One can observe that this controller is robust against such adverse conditions. However, the output feedback controller failed to provide stabilised response and is therefore not robust (results not shown).

The performance of both controllers are satisfactory under no disturbances and moderate disturbances (the

TABLE 1. Time to reach stability.

Controller	Without Dist.	Moderate Dist.	Extreme Dist.
Δ-Σ-based **1**-bit PID controller	2.75 seconds	2.75 seconds	3.2 seconds
Output Feedback Controller	1.75 seconds	3.5 seconds	Unstable

TABLE 2. Maximum overshoot.

Controller	Without Dist.	Moderate Dist.	Extreme Dist.
Δ-Σ-based single-bit PID controller	6	7.5	6
Output Feedback Controller	0.05	0.05	Unstable

results are further analysed quantitatively in Table. 1 and Table. 2). However, the output feedback controller fails to perform under extreme disturbances and limited network resources, whereas the proposed Delta-Sigma-based **1**-bit PID controller could stabilise the AUV's surge, sway and yaw velocities under extreme disturbances. Additionally, this controller uses fewer hardware and communication resources and has been demonstrated to be impervious to disturbances such as water currents.

It is worth to emphasis that, in practical systems, parametric uncertainties of the membership function are common [41]. This makes its challenging to analyse such systems with type-1 fuzzy models which contains membership functions without uncertainties. To alleviate this problem interval type-2 (IT2) fuzzy model can be used [41], [42] and is one of the subjects of the future research.

VI. CONCLUSION

This paper designed a Delta-Sigma-based **1**-bit PID controller and an output feedback controller for the land-based control of AUV systems. The design of both controllers are carried out using the Takagi-Sugeno (T-S) fuzzy representation of AUV system. The necessary conditions for stability of both these controllers are derived. The effectiveness of these controllers was investigated considering different practical maritime and networked scenarios such as moderate to high levels of disturbances; congestion attacks leading to packet losses and delay. The obtained results indicate that the proposed Delta-Sigma-based **1**-bit PID controller performance better than the output feedback controller and is robust under limited communication resources and extreme disturbances.

REFERENCES

[1] Z. Ye, D. Zhang, J. Cheng, and Z.-G. Wu, "Event-triggering and quantized sliding mode control of UMV systems under DoS attack," *IEEE Trans. Veh. Technol.*, vol. 71, no. 8, pp. 8199–8211, Aug. 2022.

[2] P. Danielis, H. Parzyjegla, M. A. M. Ali, and F. S. Torres, "Simulation model for energy consumption and acoustic underwater communication of autonomous underwater vehicles," *WMU J. Maritime Affairs*, vol. 21, no. 1, pp. 89–107, Mar. 2022.

[3] X. Liu, M. Zhang, and E. Rogers, "Trajectory tracking control for autonomous underwater vehicles based on fuzzy re-planning of a local desired trajectory," *IEEE Trans. Veh. Technol.*, vol. 68, no. 12, pp. 11657–11667, Dec. 2019.

[4] L. Qiao and W. Zhang, "Trajectory tracking control of AUVs via adaptive fast nonsingular integral terminal sliding mode control," *IEEE Trans. Ind. Informat.*, vol. 16, no. 2, pp. 1248–1258, Feb. 2020.

[5] N. Wang, Y. Gao, H. Zhao, and C. K. Ahn, "Reinforcement learning-based optimal tracking control of an unknown unmanned surface vehicle," *IEEE Trans. Neural Netw. Learn. Syst.*, vol. 32, no. 7, pp. 3034–3045, Jul. 2021.

[6] Z. Peng, Y. Jiang, and J. Wang, "Event-triggered dynamic surface control of an underactuated autonomous surface vehicle for target enclosing," *IEEE Trans. Ind. Electron.*, vol. 68, no. 4, pp. 3402–3412, Apr. 2021.

[7] Z. Peng, L. Liu, and J. Wang, "Output-feedback flocking control of multiple autonomous surface vehicles based on data-driven adaptive extended state observers," *IEEE Trans. Cybern.*, vol. 51, no. 9, pp. 4611–4622, Sep. 2021.

[8] S. Yüksel and T. Basar, "Control over noisy forward and reverse channels," *IEEE Trans. Autom. Control*, vol. 56, no. 5, pp. 1014–1029, May 2011.

[9] Z. Wang, B. Shen, H. Shu, and G. Wei, "Quantized H_∞ control for nonlinear stochastic time-delay systems with missing measurements," *IEEE Trans. Autom. Control*, vol. 57, no. 6, pp. 1431–1444, Jun. 2012.

[10] U. Premaratne, S. K. Halgamuge, and I. M. Y. Mareels, "Event triggered adaptive differential modulation: A new method for traffic reduction in networked control systems," *IEEE Trans. Autom. Control*, vol. 58, no. 7, pp. 1696–1706, Jul. 2013.

[11] D. Almakhles, A. K. Swain, A. Nasiri, and N. Patel, "An adaptive two-level quantizer for networked control systems," *IEEE Trans. Control Syst. Technol.*, vol. 25, no. 3, pp. 1084–1091, May 2017.

[12] K. Tanaka, T. Ikeda, and H. O. Wang, "Robust stabilization of a class of uncertain nonlinear systems via fuzzy control: Quadratic stabilizability, H_∞ control theory, and linear matrix inequalities," *IEEE Trans. Fuzzy Syst.*, vol. 4, no. 1, pp. 1–13, Feb. 1996.

[13] Z. Yan, J. Zhang, and G. Hu, "A new approach to fuzzy output feedback controller design of continuous-time Takagi–Sugeno fuzzy systems," *Int. J. Fuzzy Syst.*, vol. 22, no. 7, pp. 2223–2235, 2020.

[14] Z. Wang, Y. Zhao, H. Du, and K. Cao, "Stability analysis of T–S fuzzy control systems subject to actuator saturation," *Int. J. Fuzzy Syst.*, vol. 21, no. 8, pp. 2625–2631, 2019.

[15] A. K. I. Ahammed and M. F. Azeem, "Robust stabilization and control of Takagi–Sugeno fuzzy systems with parameter uncertainties and disturbances via state feedback and output feedback," *Int. J. Fuzzy Syst.*, vol. 21, no. 8, pp. 2556–2574, 2019.

[16] A. Nasiri, S. K. Nguang, A. Swain, and D. J. Almakhles, "Reducing conservatism in an H_∞ robust state-feedback control design of T–S fuzzy systems: A nonmonotonic approach," *IEEE Trans. Fuzzy Syst.*, vol. 26, no. 1, pp. 386–390, Feb. 2018.

[17] L.-Y. Hao, H. Zhang, T.-S. Li, B. Lin, and C. L. P. Chen, "Fault tolerant control for dynamic positioning of unmanned marine vehicles based on T-S fuzzy model with unknown membership functions," *IEEE Trans. Veh. Technol.*, vol. 70, no. 1, pp. 146–157, Jan. 2021.

[18] Y. Wang, B. Jiang, Z.-G. Wu, S. Xie, and Y. Peng, "Adaptive sliding mode fault-tolerant fuzzy tracking control with application to unmanned marine vehicles," *IEEE Trans. Syst., Man, Cybern., Syst.*, vol. 51, no. 11, pp. 6691–6700, Nov. 2021.

[19] Y. Zhou, G. Cheng, and S. Yu, "An SDN-enabled proactive defense framework for DDoS mitigation in IoT networks," *IEEE Trans. Inf. Forensics Security*, vol. 16, pp. 5366–5380, 2021.

[20] Z. Pan, L. Wang, Y. Wang, and Y. Liu, "Product quantization with dual codebooks for approximate nearest neighbor search," *Neurocomputing*, vol. 401, pp. 59–68, Aug. 2020.

[21] X. Shao and Y. Shi, "Neural adaptive control for MEMS gyroscope with full-state constraints and quantized input," *IEEE Trans. Ind. Informat.*, vol. 16, no. 10, pp. 6444–6454, Oct. 2020.

[22] B. Zheng and G. Yang, "Quantized output feedback stabilization of uncertain systems with input nonlinearities via sliding mode control," *Int. J. Robust Nonlinear Control*, vol. 24, no. 2, pp. 228–246, Jan. 2014.
[23] Y. Niu and D. W. C. Ho, "Control strategy with adaptive quantizer's parameters under digital communication channels," *Automatica*, vol. 50, no. 10, pp. 2665–2671, Oct. 2014.
[24] S. Dong, Z.-G. Wu, P. Shi, H. Su, and T. Huang, "Quantized control of Markov jump nonlinear systems based on fuzzy hidden Markov model," *IEEE Trans. Cybern.*, vol. 49, no. 7, pp. 2420–2430, Jul. 2019.
[25] M. Zhang, P. Shi, L. Ma, J. Cai, and H. Su, "Network-based fuzzy control for nonlinear Markov jump systems subject to quantization and dropout compensation," *Fuzzy Sets Syst.*, vol. 371, pp. 96–109, Sep. 2019.
[26] D. Liberzon, "On stabilization of linear systems with limited information," *IEEE Trans. Autom. Control*, vol. 48, no. 2, pp. 304–307, Feb. 2003.
[27] C. Wanigasekara, A. Swain, D. Almakhles, and L. Zhou, "Design of delta–sigma-based PID controller for networked wind energy conversion systems," *IEEE Trans. Ind. Appl.*, vol. 58, no. 1, pp. 879–889, Jan./Feb. 2022.
[28] C. Wanigasekara, L. Zhang, A. Swain, and S. K. Nguang, "Delta-modulator-based quantised state feedback controller for T–S fuzzy networked systems," *Int. J. Fuzzy Syst.*, vol. 23, no. 3, pp. 642–656, 2021.
[29] D. Almakhles, C. Wanigasekara, A. Swain, K. Almustafa, and U. Subramaniyan, "Hybrid delta modulator: Stability analysis using sliding mode theory," *Syst. Sci. Control Eng.*, vol. 7, no. 1, pp. 234–242, Jan. 2019.
[30] D. Almakhles, C. Wanigasekara, and A. Swain, "Delta modulator based quantised state-feedback control of networked linear systems," *IEEE Access*, vol. 10, pp. 48865–48874, 2022.
[31] D. Almakhles, A. K. Swain, and A. Nasiri, "The dynamic behaviour of data-driven Δ-M and $\Delta\Sigma$-M in sliding mode control," *Int. J. Control*, vol. 90, no. 11, pp. 2406–2414, Nov. 2017.
[32] D. J. Almakhles, A. K. Swain, and N. D. Patel, "Stability and performance analysis of bit-stream-based feedback control systems," *IEEE Trans. Ind. Electron.*, vol. 62, no. 7, pp. 4319–4327, Jul. 2015.
[33] C. Wanigasekara, D. Almakhles, A. Swain, and S. K. Nguang, "Delta-modulator-based quantised output feedback controller for linear networked control systems," *IEEE Access*, vol. 8, pp. 175169–175179, 2020.
[34] Y.-L. Wang, Q.-L. Han, M.-R. Fei, and C. Peng, "Network-based T–S fuzzy dynamic positioning controller design for unmanned marine vehicles," *IEEE Trans. Cybern.*, vol. 48, no. 9, pp. 2750–2763, Sep. 2018.
[35] C. Wanigasekara, D. Almakhles, A. Swain, S. K. Nguang, U. Subramaniyan, and S. Padmanaban, "Performance of neural network based controllers and $\Delta\Sigma$-based PID controllers for networked control systems: A comparative investigation," in *Proc. IEEE Int. Conf. Environ. Electr. Eng. IEEE Ind. Commercial Power Syst. Eur. (EEEIC/ICPS Europe)*, Jun. 2019, pp. 1–6.
[36] N. Patel, S. Nguang, G. Coghill, and A. Swain, "Online implementation of servo controllers using bit-streams," in *Proc. IEEE Region 10 Conf. (TENCON)*, Nov. 2005, pp. 1–6.
[37] K. Cao, X. Gao, H. K. Lam, and A. Vasilakos, "H_∞ fuzzy PID control synthesis for Takagi–Sugeno fuzzy systems," *IET Control Theory Appl.*, vol. 10, pp. 607–616, Apr. 2016.
[38] Q. Tran Dinh, S. Gumussoy, W. Michiels, and M. Diehl, "Combining convex–concave decompositions and linearization approaches for solving BMIs, with application to static output feedback," *IEEE Trans. Autom. Control*, vol. 57, no. 6, pp. 1377–1390, Jun. 2012.
[39] D. Huang and S. K. Nguang, "Static output feedback controller design for fuzzy systems: An ILMI approach," *Inf. Sci.*, vol. 177, no. 14, pp. 3005–3015, 2007.
[40] M. Saravanan, R. Sukumaran, M. R. Christhuraj, and T. T. Manikandan, "Delay in underwater acoustic wireless single channel communication: Stochastic network calculus," in *Proc. 4th Int. Conf. I-SMAC (IoT Social, Mobile, Analytics Cloud) (I-SMAC)*, Oct. 2020, pp. 1138–1144.
[41] Z. Gu, D. Yue, J. H. Park, and X. Xie, "Memory-event-triggered fault detection of networked IT2 T–S fuzzy systems," *IEEE Trans. Cybern.*, vol. 53, no. 2, pp. 743–752, Feb. 2023.
[42] Y. Yang, Y. Niu, and J. Lam, "Security interval type-2 fuzzy sliding mode control under multistrategy injection attack: Design, analysis, and optimization," *IEEE Trans. Fuzzy Syst.*, vol. 31, no. 9, pp. 2943–2955, Sep. 2023.

CHATHURA WANIGASEKARA (Member, IEEE) received the B.Sc. (Eng.) degree in electrical and electronic engineering from the University of Peradeniya, Sri Lanka, in 2013, and the Master of Engineering degree in electrical and electronic engineering and the Ph.D. degree in control engineering from The University of Auckland, New Zealand, in 2016 and 2020, respectively.

He is currently a Control/Systems Engineer with the Institute for the Protection of Maritime Infrastructures, German Aerospace Centre, Bremerhaven, Germany. He is also a Lecturer with the University of Bremen, Germany, where he was a Postdoctoral Researcher with the Centre for Industrial Mathematics, from 2020 to 2022. His current research interests include nonlinear system identification and control, machine learning, and networked control systems. He was a recipient of the Fowlds Memorial Prize for the most distinguished student in Master of Engineering, in 2016.

FRANK SILL TORRES (Senior Member, IEEE) received the Diploma and Dr.-Ing. degrees in electrical engineering from the University of Rostock, Germany, in 2002 and 2007, respectively. From 2007 to 2010, he was a Postdoctoral Fellow with the Federal University of Minas Gerais (UFMG), Brazil. From 2010 to 2018, he was a Professor with the Department of Electronic Engineering, UFMG, where he also coordinated the ASIC Reliability Group. From 2018 to 2019, he was with the German Research Center for Artificial Intelligence (DFKI), Bremen, Germany. Since 2019, he has been the Head of the Department for Resilience of Maritime Socio-technical Systems at the Institute for the Protection of Maritime Infrastructures of the German Aerospace Center (DLR), Bremerhaven, Germany. Since 2021, he holds additionally the position as Acting Institute Director of this institute. He is a lecturer at the University of Bremen, Germany and UAS, Bremerhaven. His primary research interests include resilience, maritime security, and emerging technologies. He is the author and coauthor of more than 150 scientific publications and three books and holds two patents. He was a member of several conference committees and an Associate Researcher of the Brazilian National Research Council (CNPq).

AKSHYA SWAIN (Senior Member, IEEE) received the B.Sc. (Eng.) (Hons.) and M.E. degrees, in 1985 and 1988, respectively, and the Ph.D. degree in control engineering from The University of Sheffield, in 1996. He is currently an Associate Editor of IEEE SENSORS JOURNAL and *International Journal of Innovative Computing, Information and Control*, an Editor of *Electronics* (MDPI), and a member of the Editorial Board of *International Journal of Automation and Control* and *International Journal of Sensors and Wireless Communications and Control*. His current research interests include nonlinear system identification and control, machine learning, and big data.